



Interferometry with Bose-Einstein Condensates in Microgravity

H. Müntinga,¹ H. Ahlers,² M. Krutzik,³ A. Wenzlawski,⁴ S. Arnold,⁵ D. Becker,² K. Bongs,⁶ H. Dittus,⁷ H. Duncker,⁴ N. Gaaloul,² C. Gherasim,⁸ E. Giese,⁵ C. Grzeschik,³ T. W. Hänsch,⁹ O. Hellmig,⁴ W. Herr,² S. Herrmann,¹ E. Kajari,^{5,10} S. Kleinert,⁵ C. Lämmerzahl,¹ W. Lewoczko-Adamczyk,³ J. Malcolm,⁶ N. Meyer,⁶ R. Nolte,⁸ A. Peters,^{3,11} M. Popp,² J. Reichel,¹² A. Roura,⁵ J. Rudolph,² M. Schiemangk,^{3,11} M. Schneider,⁸ S. T. Seidel,² K. Sengstock,⁴ V. Tamma,⁵ T. Valenzuela,⁶ A. Vogel,⁴ R. Walser,⁸ T. Wendrich,² P. Windpassinger,⁴ W. Zeller,⁵ T. van Zoest,⁷ W. Ertmer,² W. P. Schleich,⁵ and E. M. Rasel^{2,*}

¹ZARM, Universität Bremen, Am Fallturm, 28359 Bremen, Germany

²Institut für Quantenoptik, Leibniz Universität Hannover, Welfengarten 1, 30167 Hannover, Germany

³Institut für Physik, Humboldt-Universität zu Berlin, Newtonstraße 15, 12489 Berlin, Germany

⁴Institut für Laser-Physik, Universität Hamburg, Luruper Chaussee 149, 22761 Hamburg, Germany

⁵Institut für Quantenphysik and Center for Integrated Quantum Science and Technology (IQST), Universität Ulm, Albert-Einstein-Allee 11, 89081 Ulm, Germany

⁶Midlands Ultracold Atom Research Centre, Birmingham B15 2TT, United Kingdom

⁷DLR Institut für Raumfahrtssysteme, Robert-Hooke-Straße 7, 28359 Bremen, Germany

⁸Institut für Angewandte Physik, Technische Universität Darmstadt, Hochschulstraße 4A, 64289 Darmstadt, Germany

⁹Max-Planck-Institut für Quantenoptik und Fakultät für Physik der Ludwig-Maximilians-Universität München, Schellingstraße 4, 80799 München, Germany

¹⁰Theoretische Physik, Universität des Saarlandes, Campus E2 6, D-66041 Saarbrücken, Germany

¹¹Ferdinand-Braun-Institut, Leibniz-Institut für Höchstfrequenztechnik, Gustav-Kirchhoff-Straße 4, 12489 Berlin, Germany

¹²Laboratoire Kastler Brossel, ENS/UPMC-Paris 6/CNRS, 24 rue Lhomond, 75005 Paris, France

(Received 22 January 2013; published 25 February 2013)

Atom interferometers covering macroscopic domains of space-time are a spectacular manifestation of the wave nature of matter. Because of their unique coherence properties, Bose-Einstein condensates are ideal sources for an atom interferometer in extended free fall. In this Letter we report on the realization of an asymmetric Mach-Zehnder interferometer operated with a Bose-Einstein condensate in microgravity. The resulting interference pattern is similar to the one in the far field of a double slit and shows a linear scaling with the time the wave packets expand. We employ delta-kick cooling in order to enhance the signal and extend our atom interferometer. Our experiments demonstrate the high potential of interferometers operated with quantum gases for probing the fundamental concepts of quantum mechanics and general relativity.

DOI: [10.1103/PhysRevLett.110.093602](https://doi.org/10.1103/PhysRevLett.110.093602)

PACS numbers: 42.50.Gy, 03.75.Dg, 04.80.Cc, 37.25.+k

Quantum theory [1] and general relativity [2] are two pillars of modern physics and successfully describe phenomena of the micro- and the macro-cosmos, respectively. So far they have resisted any attempt of complete unification, and quantum gravity [3] is generally considered the Holy Grail of physics. Experimental tests of gravity [4] with matter waves [5] started as early as 1975 with neutrons [6,7]. Today, atom interferometers (AIs) [8] offer new opportunities to probe the interface of these fundamentally disparate descriptions of nature. The coherent evolution of quantum objects delocalized in space-time [9], the verification of the Einstein principle of equivalence with quantum objects [10], and the detection of gravitational waves [11] constitute only three of many timely quests motivating experiments with AI in extended free fall. The overarching aim is to enhance the sensitivity of these devices, which increases linearly with the momentum difference between the two matter waves [12] emerging from a beam splitter and quadratically with the time of free fall as experienced in fountains [10,13,14], drop towers [15], parabolic flights

[16], and space [17]. These scaling laws imply constraints with respect to the atomic source. Thanks to their slow spreading and their excellent mode properties, Bose-Einstein condensates (BECs) [18,19] represent a promising source [9] for high-resolution interferometers [20–22]. Moreover, atom chips have enormously simplified the generation of BECs [23–25] and paved the way to on-chip matter-wave interferometry [26,27].

In this Letter, we report on the demonstration of a BEC interferometer in microgravity. In our experiment, we employ an atom chip as a robust and fast source for feeding an interferometer with a BEC consisting of about 10^4 ^{87}Rb atoms. Taking advantage of the extended free fall provided at the drop tower of the Center of Applied Space Technology and Microgravity (ZARM) in Bremen, we have been able to coherently split the BEC and to separate the emerging wave packets over macroscopic scales in time and space. The interferometer extends over more than half a second and covers distances of millimeters, exceeding the width of the condensate by an order of

magnitude. By applying delta-kick cooling (DKC) [28–30] we have been able to reduce the expansion and to enhance the signal at longer interferometry times. We study the coherent evolution of the BEC for increasing temporal and spatial separation of the wave packets inside the interferometer by monitoring the single-shot contrast and shape of the fringes [31].

Our experiments are performed with an asymmetric Mach-Zehnder interferometer (AMZI) [20,32] shown in Fig. 1. Here we display the temporal evolution of the atomic density distribution of the BEC interferometer for an experiment on ground [Fig. 1(a)] and the corresponding experimental sequence for forming the interferometer [Fig. 1(b)]. A macroscopic wave packet is coherently split, redirected, and brought to a partial overlap by successive Bragg scattering at moving light crystals [26,33,34]. They are generated by pulses of two counter-propagating laser beams separated by the two-photon recoil energy of 15 kHz and detuned from the $F = 2 \rightarrow F = 3$ transition of the D_2 line of ^{87}Rb by 800 MHz to reduce spontaneous scattering. There exists a close analogy to the Young double-slit experiment [Fig. 1(c)], where one pair of overlapping BECs plays the role of a pair of coherent light waves emanating from two slits separated by a distance d . Similar to the resulting interference pattern in the far field of the double slit,

the fringe spacing in our expanding cloud, being the distance between two local maxima of the density, increases with the total expansion time T_{ex} of the BEC and is inversely proportional to the displacement d of the two clouds.

Figure 2 illustrates our experiments in microgravity performed at the drop tower. We show the complete temporal sequence [Fig. 2(a)], which differs from the previous experiments with the apparatus [15] in three important features: (i) We employ DKC to reduce the expansion during the free fall by briefly (2 ms) switching on the trap with frequencies of (10, 22, 27) Hz generated by the atom chip 30 ms after the release. (ii) In order to eliminate detrimental effects of residual magnetic fields we transfer the BEC into the nonmagnetic state $|F = 2, m_F = 0\rangle$ by coupling the Zeeman levels with a chirped radio-frequency pulse (adiabatic rapid passage) [35]. (iii) At the time T_0 after the release of the BEC, we implement the sequence of the AMZI outlined in Fig. 1 and detect the interference pattern at T_{ex} after the release using absorption imaging with a single laser pulse as illustrated in Fig. 2(b). In Fig. 2(c) we show typical images of the interfering BECs and the corresponding column density profiles for two different values of T_{ex} .

Figure 3 summarizes the central results of our Letter on probing the coherent evolution of a BEC with an

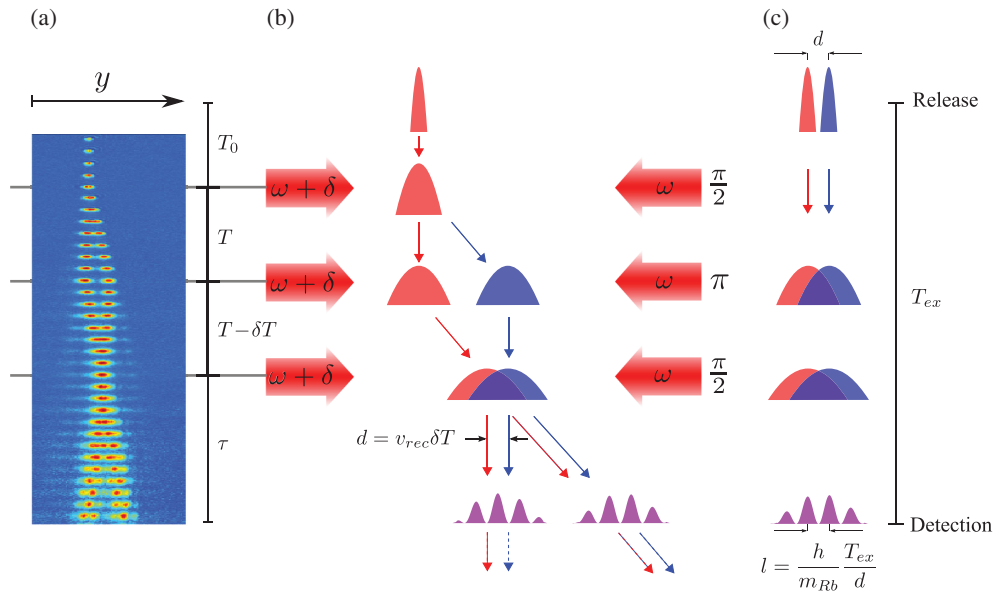


FIG. 1 (color). Temporal AMZI for a BEC based on Bragg scattering at a light grating: experimental images on ground (a), schematic sequence (b), and analogy to the Young double-slit experiment (c). The evolution of the BEC and the AMZI is visualized by a series of absorption images (a) of the atomic densities separated by 1 ms. The incomplete transfer is a consequence of the larger mean-field energy of the BEC necessary for the ground experiment. The interferometer starts at the time T_0 after the release of the BEC, when a $\pi/2$ pulse (b) made out of two counter-propagating light beams of frequency ω and $\omega + \delta$ creates a coherent superposition of two wave packets that drift apart with the two-photon recoil velocity $v_{\text{rec}} = 11.8$ mm/s. After T they are redirected by a π pulse and partially recombined after $T - \delta T$ by a second $\pi/2$ pulse. A nonzero value of δT leads to a spatial interference pattern, which we record after $\tau = 53$ ms in free fall. Similar to the far-field pattern observed in the Young double-slit experiment (c), the fringe spacing l scales linearly with the time of expansion $T_{\text{ex}} = T_0 + 2T - \delta T + \tau$ and is inversely proportional to the separation $d = v_{\text{rec}} \delta T$ of the wave packets. The scaling factor is the ratio of Planck's constant h and the mass m_{Rb} of the Rubidium atoms.

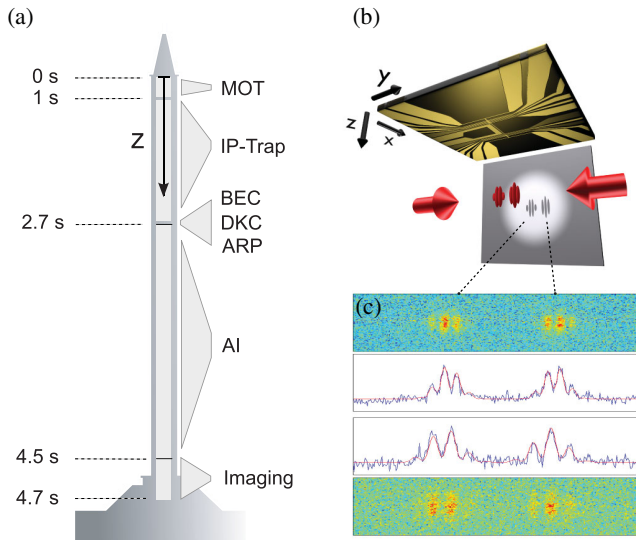


FIG. 2 (color). Mach-Zehnder interferometry of a BEC in microgravity as realized in the ZARM drop tower in Bremen (a) where absorption imaging (b) brings out the interference fringes (c). The preparatory experimental sequence (a) includes capturing cold atoms in a magneto-optical trap (MOT), loading an Ioffe-Pritchard trap, creating a BEC, and applying the DKC followed by the adiabatic rapid passage (ARP). The remaining time before the capture of the capsule at the bottom of the tower is used for AI and imaging of the atoms. The AMZI below the atom chip [top plane of (b)] is formed by scattering the BEC off moving Bragg gratings generated by two counter-propagating laser beams (red arrows directed along the y axis), resulting in two pairs of interfering BECs. A resonant laser beam propagating along the x axis projects the shadow of the BEC onto a CCD camera. Typical interference patterns and the corresponding column densities (c) are shown for T_{ex} of 180 and 260 ms with corresponding fringe spacing of 75 and 107 μm .

interferometer in extended free fall. It shows the spatial period of the observed fringe pattern [Fig. 3(a)] as a function of the expansion time T_{ex} , and the contrast [Fig. 3(b)] observed at the exit ports of the AI for increasing values $2T - \delta T$ of the time the BEC spends in the interferometer. Moreover, in Fig. 3(a) we confront the experimental results (blue circles, red squares, black triangles) with the corresponding theoretical predictions (solid blue and red lines). The solid blue line originates from a model based on the scaling approach [36–39] and describes the interference pattern of two condensates initially separated by a distance d , which start to expand and eventually overlap. Their initial shape is derived from a detailed numerical model of our magnetic chip trap. For large time scales the observed fringe spacing (blue dots) shows a linear increase with T_{ex} in full accordance with our model and with the linear far-field prediction (dash-dotted blue curve) of the double slit. We emphasize that our microgravity experiments operate deep in the linear regime and the nonlinear behavior typical for the near field

combined with the nonlinear evolution of the BEC occurs only at very short times (< 30 ms). The linear scaling of the fringe pattern confirms the unperturbed evolution of the BEC during extended free fall.

The expansion rate of the BEC due to the mean-field energy is a limiting factor for extending the interferometer to even longer time scales. It can be reduced by DKC, which acts on the BEC like a three-dimensional lens. Indeed, in our experiments DKC realized with the atom chip eliminates a substantial part of the kinetic energy of the BEC, giving rise to an effective temperature of about 1 nK. The method allows us to extend the observation of the free evolution of the BEC and was tested with our AMZI. The experimental observations (red squares) of the fringe spacing agree well with the theoretical predictions (solid red line) for a double-slit experiment with delta-kick cooled atoms. In order to reach even longer times (black triangles), we have adjusted the detection time τ such that the patterns of the two exit ports overlap, thus increasing the absorption signal.

As shown in Fig. 3(b), we observe a contrast of more than 40%, even at times $2T - \delta T$ as large as half a second. However, then the contrast decreases with the time over which the wave packets are separated, and generally with the expansion time of the BEC. The observed reduction is nonexponential in time and uniform over the cloud. In this respect the asymmetric interferometer puts more severe constraints on the setup than the symmetric one. However, it allows us to analyze various effects perturbing the interferometer. A preliminary analysis shows that the reduction may be due to an imperfect alignment of the beam splitters, inhomogeneous wave fronts or disturbances resulting from a slight capsule rotation. A more detailed discussion is subject to future investigations.

In conclusion, our device represents a unique test bed for exploring atom interferometry with novel states of matter in extended free fall. In particular, it allows us to test tools of atom optics, such as the precise mode control of a BEC with DKC at energy scales approaching pK temperatures. These concepts are essential for high-resolution measurements both in fountains and in microgravity.

Moreover, in our experiment we could follow the evolution of the temporal coherence of an asymmetric Mach-Zehnder interferometer with a BEC in microgravity, which is analogous to Young’s double-slit experiment with a gigantic matter-wave packet being in free fall for nearly a second. All preparatory steps necessary for high-precision interferometry are implemented with the help of a robust chip-based BEC source.

Employing our present setup with a stabilized phase as an accelerometer, the number of condensed atoms would compromise the gain in resolution due to the extended time in the interferometer. We expect that the next generation of our setup will provide us with a BEC consisting of 10^6 particles, improved DKC and techniques to correct for

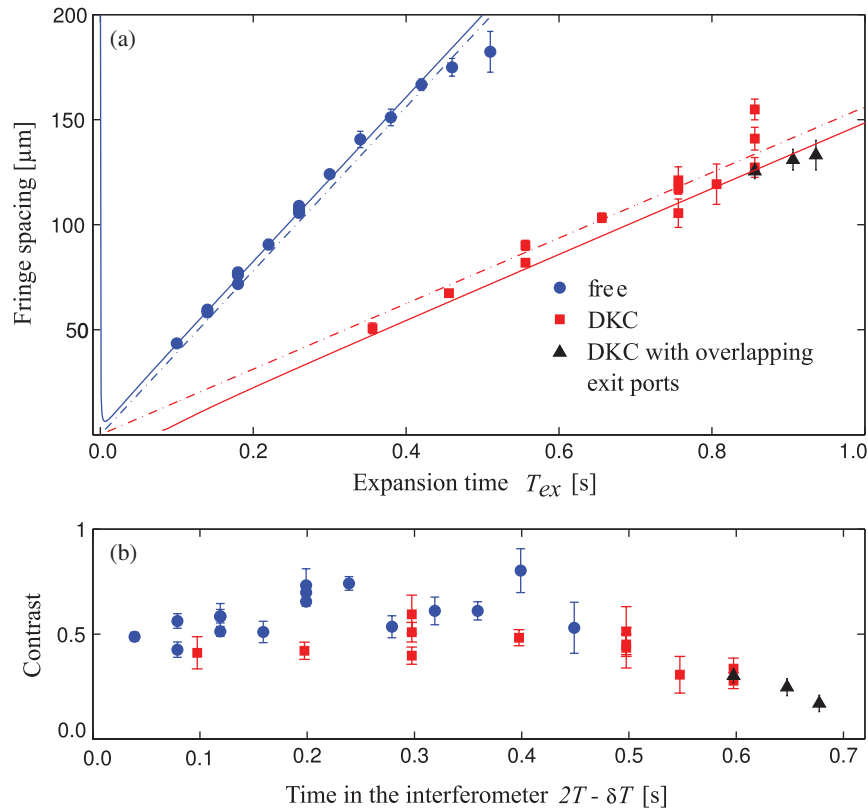


FIG. 3 (color). Fringe spacing (a) of two interfering BECs observed at each exit port of an AMZI with (red squares, black triangles, solid red line) and without (blue dots, solid blue line) DKC as a function of the expansion time T_{ex} , and contrast (b) in its dependence on the time $2T - \delta T$ spent in the interferometer. Our data (blue dots, red boxes, black triangles) agree well with our models of free expansion (solid blue line) and DKC (solid red line). In the case of DKC, the temporal asymmetry δT was increased from 1 to 2.5 ms in order to preserve the number of visible fringes across the smaller BEC by rescaling the fringes, which decreased the slope in (a). With and without DKC, the observed linear dependence has the slope of the approximation of the double slit for point particles (dash-dotted lines). An offset arises from the initial size and the nonlinear expansion of the BEC due to mean-field energy or from the focusing in DKC, which shifts the apparent location of the double slit to earlier or later times, respectively. The high contrast of the interference fringes (b), obtained by absorption imaging, typically exceeds 40% but fades away for increasing T . Error bars depict 1- σ -confidence bounds of the fitted parameters.

inertial perturbations. The sensitivity achievable with this device will strongly depend on the control of decoherence mechanisms, which we will further explore. Its operation in the drop tower or the catapult allows for free-fall times of 4.7 or 9.4 s corresponding to a shot-noise limited resolution of $6.2 \times (10^{-11} \text{ m/s}^2)$ or $5.5 \times (10^{-12} \text{ m/s}^2)$, respectively. Indeed, a fountainlike interferometer would need more than hundred meters to achieve the time of free fall provided by the catapult at the ZARM. Last but not least, our source is currently considered for implementing quantum tests of the weak equivalence principle on sounding rockets, the International Space Station, and satellite missions. We emphasize that the limit of our future device will already be close to the one targeted by recently proposed space missions such as STE-QUEST [40].

H. M., A. H., M. K., and A. W. contributed equally to this work. This project is supported by the German Space Agency (DLR) with funds provided by the Federal

Ministry of Economics and Technology (BMWi) due to an enactment of the German Bundestag under Grant No. DLR 50WM1131-1137 (project QUANTUS-III). The authors also thank the German Research Foundation (DFG) for funding the Cluster of Excellence QUEST Centre for Quantum Engineering and Space-Time Research.

*To whom correspondence should be addressed.

rasel@iqo.uni-hannover.de

- [1] D. Bohm, *Quantum Theory* (Prentice Hall, Englewood Cliffs, 1951).
- [2] C. W. Misner, K. S. Thorne, and J. A. Wheeler, *Gravitation* (W. H. Freeman, San Francisco, 1973).
- [3] C. Kiefer, *Quantum Gravity* (Oxford University Press, Oxford, 2007).
- [4] C. M. Will, *Living Rev. Relativity* **9**, 3 (2006), <http://www.livingreviews.org/lrr-2006-3>.

- [5] P. R. Berman, *Atom Interferometry* (Academic Press, San Diego, CA, 1997).
- [6] R. Colella, A. W. Overhauser, and S. A. Werner, *Phys. Rev. Lett.* **34**, 1472 (1975).
- [7] H. Rauch and S. Werner, *Neutron Interferometry: Lessons in Experimental Quantum Mechanics* (Oxford University Press, Oxford, 2000).
- [8] A. D. Cronin, J. Schmiedmayer, and D. E. Pritchard, *Rev. Mod. Phys.* **81**, 1051 (2009).
- [9] B. Lamine, R. Hervé, A. Lambrecht, and S. Reynaud, *Phys. Rev. Lett.* **96**, 050405 (2006).
- [10] S. Dimopoulos, P. W. Graham, J. M. Hogan, and M. A. Kasevich, *Phys. Rev. Lett.* **98**, 111102 (2007).
- [11] S. Dimopoulos, P. W. Graham, J. M. Hogan, M. A. Kasevich, and S. Rajendran, *Phys. Rev. D* **78**, 122002 (2008).
- [12] S.-w. Chiow, T. Kovachy, H.-C. Chien, and M. A. Kasevich, *Phys. Rev. Lett.* **107**, 130403 (2011).
- [13] H. Müller, S.-w. Chiow, S. Herrmann, S. Chu, and K.-Y. Chung, *Phys. Rev. Lett.* **100**, 031101 (2008).
- [14] S. Dickerson, J. Hogan, A. Sugarbaker, and M. Kasevich, Atom Interferometry in a 10 m Tower, <http://www.pqeconference.com/pqe2013/abstractd/018p.pdf>.
- [15] T. van Zoest *et al.*, *Science* **328**, 1540 (2010).
- [16] R. Geiger *et al.*, *Nat. Commun.* **2**, 474 (2011).
- [17] E. Arimondo, W. Ertmer, W. Schleich, and E. M. Rasel, *Atom Optics and Space Physics: Proceedings of the International School of Physics “Enrico Fermi”* (IOS Press, Bologna, Italy, 2009).
- [18] E. A. Cornell and C. E. Wieman, *Rev. Mod. Phys.* **74**, 875 (2002).
- [19] W. Ketterle, *Rev. Mod. Phys.* **74**, 1131 (2002).
- [20] Y. Torii, Y. Suzuki, M. Kozuma, T. Sugiura, T. Kuga, L. Deng, and E. W. Hagley, *Phys. Rev. A* **61**, 041602 (2000).
- [21] J. E. Simsarian, J. Denschlag, M. Edwards, C. W. Clark, L. Deng, E. W. Hagley, K. Helmerson, S. L. Rolston, and W. D. Phillips, *Phys. Rev. Lett.* **85**, 2040 (2000).
- [22] J. E. Debs, P. A. Altin, T. H. Barter, D. Döring, G. R. Dennis, G. McDonald, R. P. Anderson, J. D. Close, and N. P. Robins, *Phys. Rev. A* **84**, 033610 (2011).
- [23] W. Hänsel, P. Hommelhoff, T. W. Hänsch, and J. Reichel, *Nature (London)* **413**, 498 (2001).
- [24] R. Folman, P. Krüger, J. Schmiedmayer, J. Denschlag, and C. Henkel, in *Advances in Atomic, Molecular, and Optical Physics*, edited by B. Bederson and H. Walther (Academic Press, New York, 2002), Vol. 48, pp. 263–356.
- [25] J. Fortágh and C. Zimmermann, *Rev. Mod. Phys.* **79**, 235 (2007).
- [26] Y.-J. Wang, D. Z. Anderson, V. M. Bright, E. A. Cornell, Q. Diot, T. Kishimoto, M. Prentiss, R. A. Saravanan, S. R. Segal, and S. Wu, *Phys. Rev. Lett.* **94**, 090405 (2005).
- [27] T. Schumm, S. Hofferberth, L. M. Andersson, S. Wildermuth, S. Groth, I. Bar-Joseph, J. Schmiedmayer, and P. Krüger, *Nat. Phys.* **1**, 57 (2005).
- [28] S. Chu, J. E. Bjorkholm, A. Ashkin, J. P. Gordon, and L. W. Hollberg, *Opt. Lett.* **11**, 73 (1986).
- [29] H. Ammann and N. Christensen, *Phys. Rev. Lett.* **78**, 2088 (1997).
- [30] M. Morinaga, I. Bouchoule, J.-C. Karam, and C. Salomon, *Phys. Rev. Lett.* **83**, 4037 (1999).
- [31] The position of the fringes jumps from shot to shot because we use two independent laser beams to create the light crystal. However, this feature is irrelevant for the measurements reported in our Letter. For more detailed discussions see the Supplemental Material [36].
- [32] H. Rauch, H. Wölwitsch, H. Kaiser, R. Clothier, and S. A. Werner, *Phys. Rev. A* **53**, 902 (1996).
- [33] M. Kozuma, L. Deng, E. W. Hagley, J. Wen, R. Lutwak, K. Helmerson, S. L. Rolston, and W. D. Phillips, *Phys. Rev. Lett.* **82**, 871 (1999).
- [34] K. Nakagawa and M. Horikoshi, *J. Phys. Conf. Ser.* **185**, 012031 (2009).
- [35] J. C. Camparo and R. P. Frueholz, *J. Phys. B* **17**, 4169 (1984).
- [36] See Supplemental Material at <http://link.aps.org/supplemental/10.1103/PhysRevLett.110.093602> for expansion theory and image analysis.
- [37] Y. Castin and R. Dum, *Phys. Rev. Lett.* **77**, 5315 (1996).
- [38] P. Storey and M. Olshanii, *Phys. Rev. A* **62**, 033604 (2000).
- [39] G. Nandi, R. Walser, E. Kajari, and W. P. Schleich, *Phys. Rev. A* **76**, 063617 (2007).
- [40] STE-QUEST space mission in ESA’s Cosmic Vision 2020-22, <http://sci.esa.int/ste-quest>.